Tetris-inspired detector with neural network for radiation mapping: Supplementary Information

Ryotaro Okabe[1,2,*,†], **Shangjie Xue**[1,3,4,*,†], **Jiankai Yu**[3], **Tongtong Liu**[1,5], **Benoit Forget**[3], **Stefanie Jegelka**[4], **Gordon Kohse**[6], **Lin-wen Hu**[6,†], **and Mingda Li**[1,3,†]

[1]*Quantum Measurement Group, Massachusetts Institute of Technology, Cambridge, MA 02139, USA*
[2]*Department of Chemistry, Massachusetts Institute of Technology, Cambridge, MA 02139, USA*
[3]*Department of Nuclear Science and Engineering, Massachusetts Institute of Technology, Cambridge, MA 02139, USA*
[4]*Department of Electrical Engineering and Computer Science, Massachusetts Institute of Technology, Cambridge, MA 02139, USA*
[5]*Department of Physics, Massachusetts Institute of Technology, Cambridge, MA 02139, USA*
[6]*Nuclear Reactor Laboratory, Massachusetts Institute of Technology, Cambridge, MA 02139, USA*
[*]*These authors contributed equally to this work*
[†]*Corresponding authors:* rokabe@mit.edu, lwhu@mit.edu, mingda@mit.edu

Monte Carlo Simulation Setting and Data Representation

Our radiation detectors consist of two materials: CdZnTe to absorb radiation and Pd as padding layers. The density of CdZnTe and Pd are set 5.76 g/cm^3 and 11.35 g/cm^3 respectively. Table S1 shows the MC simulation settings to generate training data and the filter layers. Figure S1 shows the position of the radiation sources used for training of S-shape detector. The 64 near-field filters of the S-shape detector are visualized in Fig. S2.

Table S1. The parameter setting for Monte-Carlo simulations for radiation source detection.

	Training, Testing Data	Filter
The number of photon particles	50000	80000
The number of angle sectors	64	64
radiation source energy [MeV]	0.5	0.5
The detector-source distance [cm]	20 $\sim$500	near: 50, far: 500
The number of simulation data	3000	64$\times$2 channels

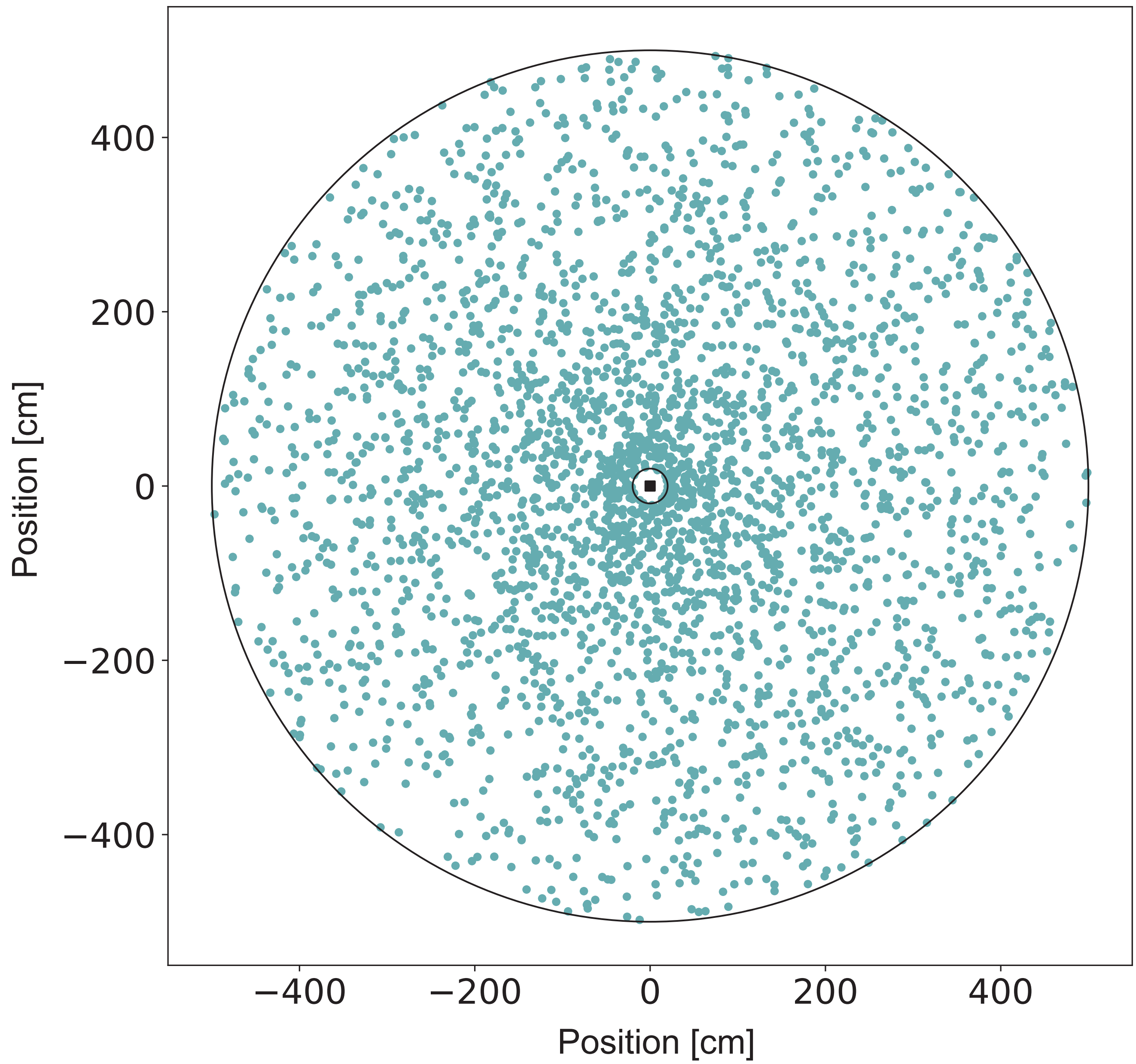

Figure S1. **Visualizations of the radiation source positions of training data.**
the black square is the detector's position. Blue dots are the radiation source positions (3,000 data). The circles shows the minimum and maximum distance between the radiation sources and the detector.

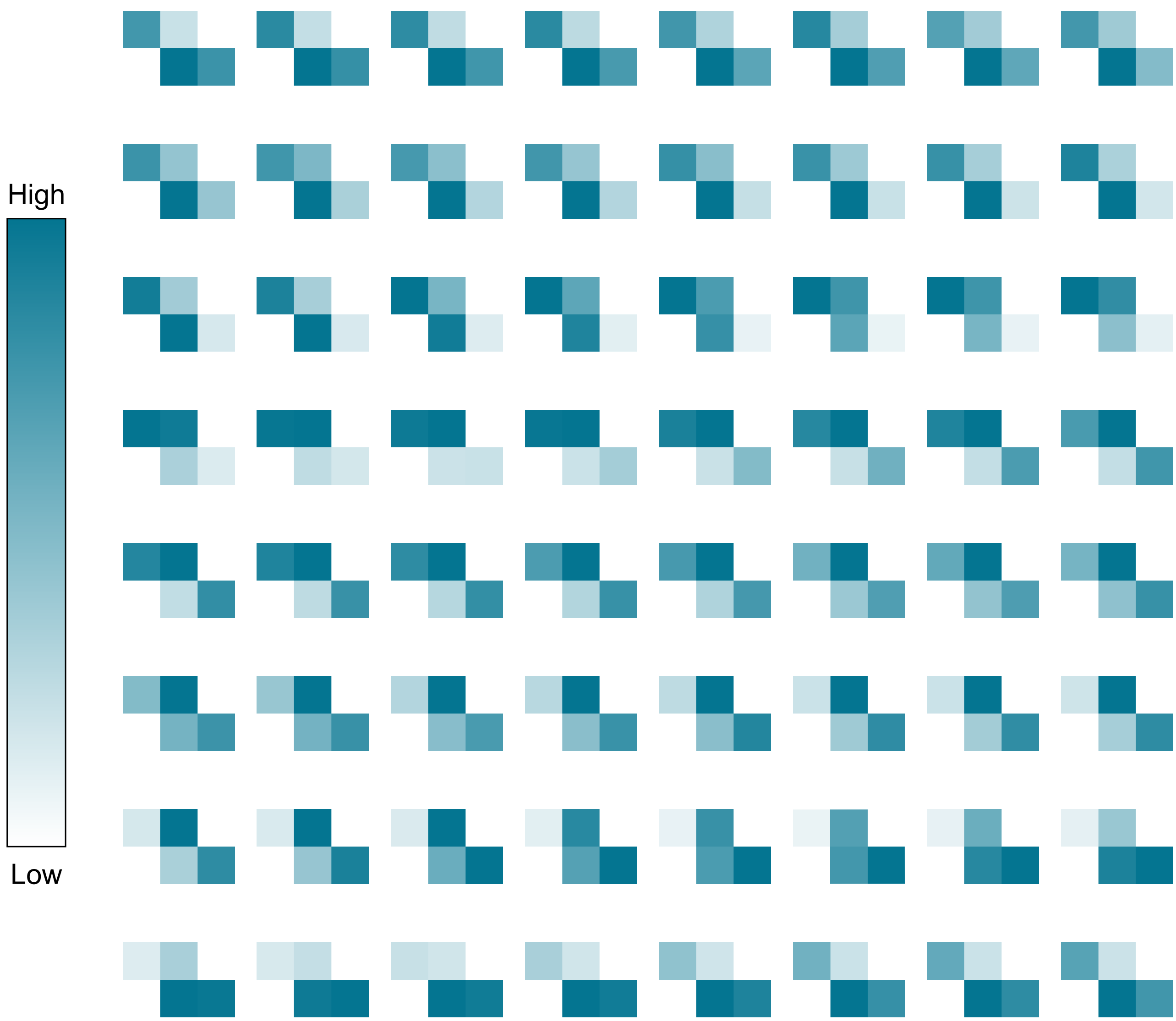

Figure S2. The near-field global filters of the S-shape configuration.
All of the 64 arrays represents the filters with a radiation source coming from different direction. As the color bar of the left side shows, the intense color represents higher input signals. We use the another set of 64 far-field filters to capture the direction of radiation sources.

Deep Neural Network Architecture

We implemented U-shaped neural network to predict the angular information from the detector's signal. The dimensions of each layer are shown in Fig. S3. The input data goes through 64 filter layers of both far- and near-field channels, and embedded as $(2,64)$ matrix. The U-net is then applied to this embedded data and output an array of 64 elements. Table S2 summarizes the hyperparameters of the U-shaped neural network.

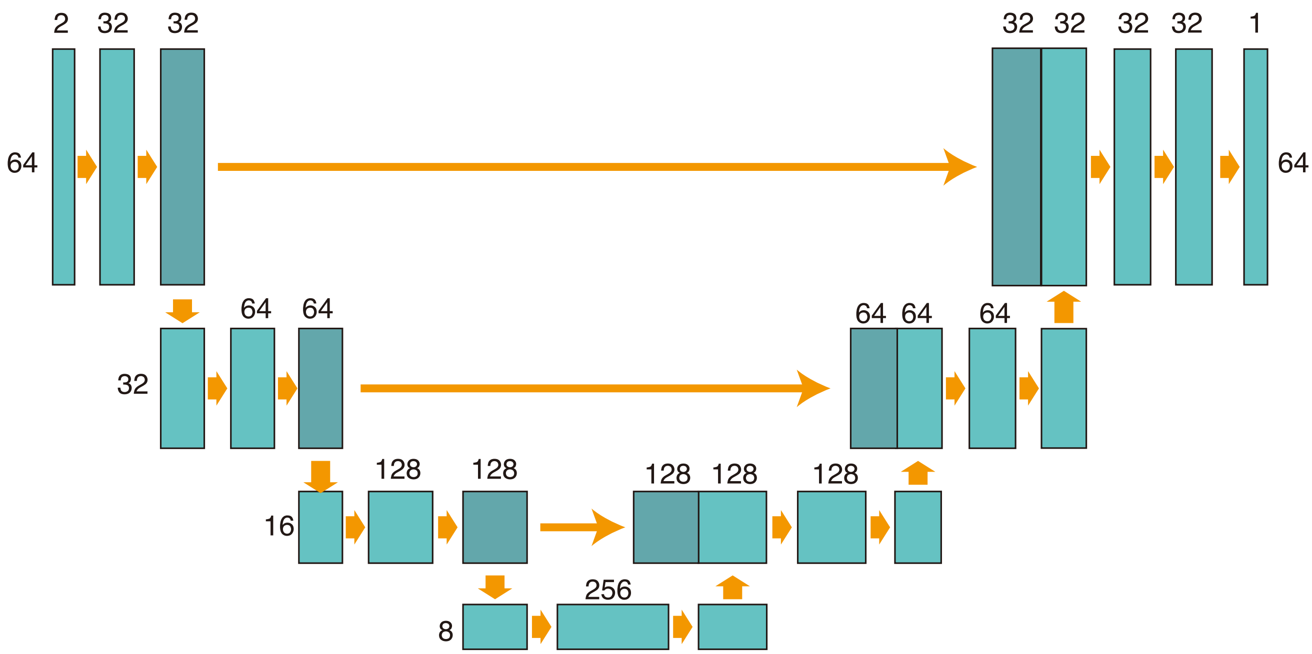

Figure S3. Model architecture of U-net convolutional neural networks.
The number near the rectangular shapes represents the digits of matrices. The model consists of convolution, transposed convolution, max pooling and concatenation.

Table S2. The parameter setting of U-net

Hyperparameter	1-source detector	2-source detector
Epochs	200	5000
The number of angle sectors	64	64
batch size	256	256
AdamW optimizer learning rate	1×10^{-3}	1×10^{-3}
AdamW optimizer weight decay coefficient	3×10^{-5}	3×10^{-5}
Training data size	2700	2700
Testing data	300	300

Radiation Source Mapping with Maximum A Posteriori (MAP) estimation

A method based on Maximum a Posteriori (MAP) Estimation is applied to generate the radiation distribution map. In the mapping process the intensity contribution of the i^{th} pixel to the j^{th} directional sector of the detector at time t is recorded. Figure S4 explains the roles of these factors in the mapping process. Using this method we have worked on single radiation source detection using detectors with four CZT panels. The result using S-shape detector, which worked the best among the other simple configurations, is shown in our main document. Figure S5-S7 illustrate the radiation mapping results with 2×2 square, J- and T-shape detectors. To track the directional prediction at each time during the mapping process, we plot the direct predictions of angles in Fig. S8. It is obvious that the fluctuation of the directional predictions at each sites reflects the performance of radiation mapping. Furthermore, we have worked on mapping two radiation sources simultaneously. Figure S9-S10 show the result using 10×10 and 5×5 square detector.

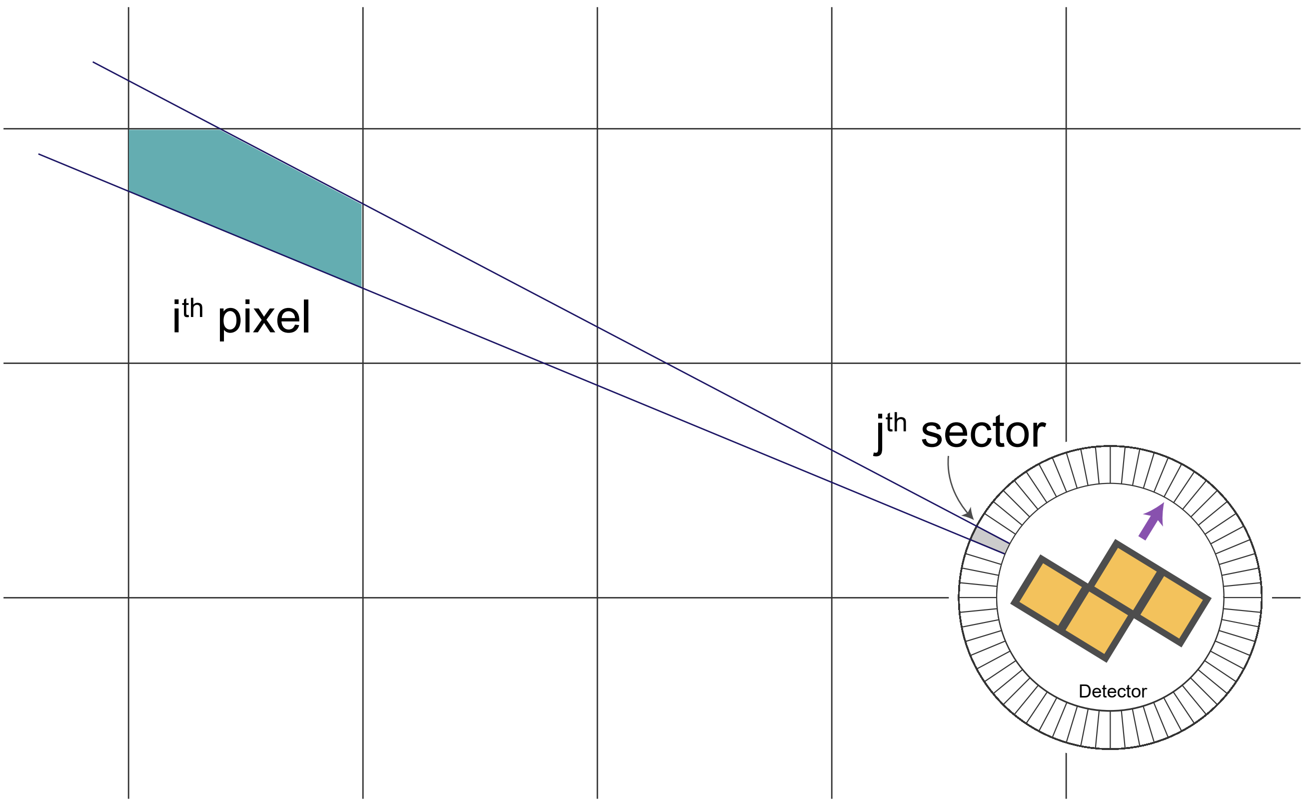

Figure S4. **An illustration of the element of the observation matrix.**
The purple arrow near the detector indicates the front side of the detector. The blue area on the grid indicates the overlapped region of the i^{th} pixel and the j^{th} sector of detection angle.

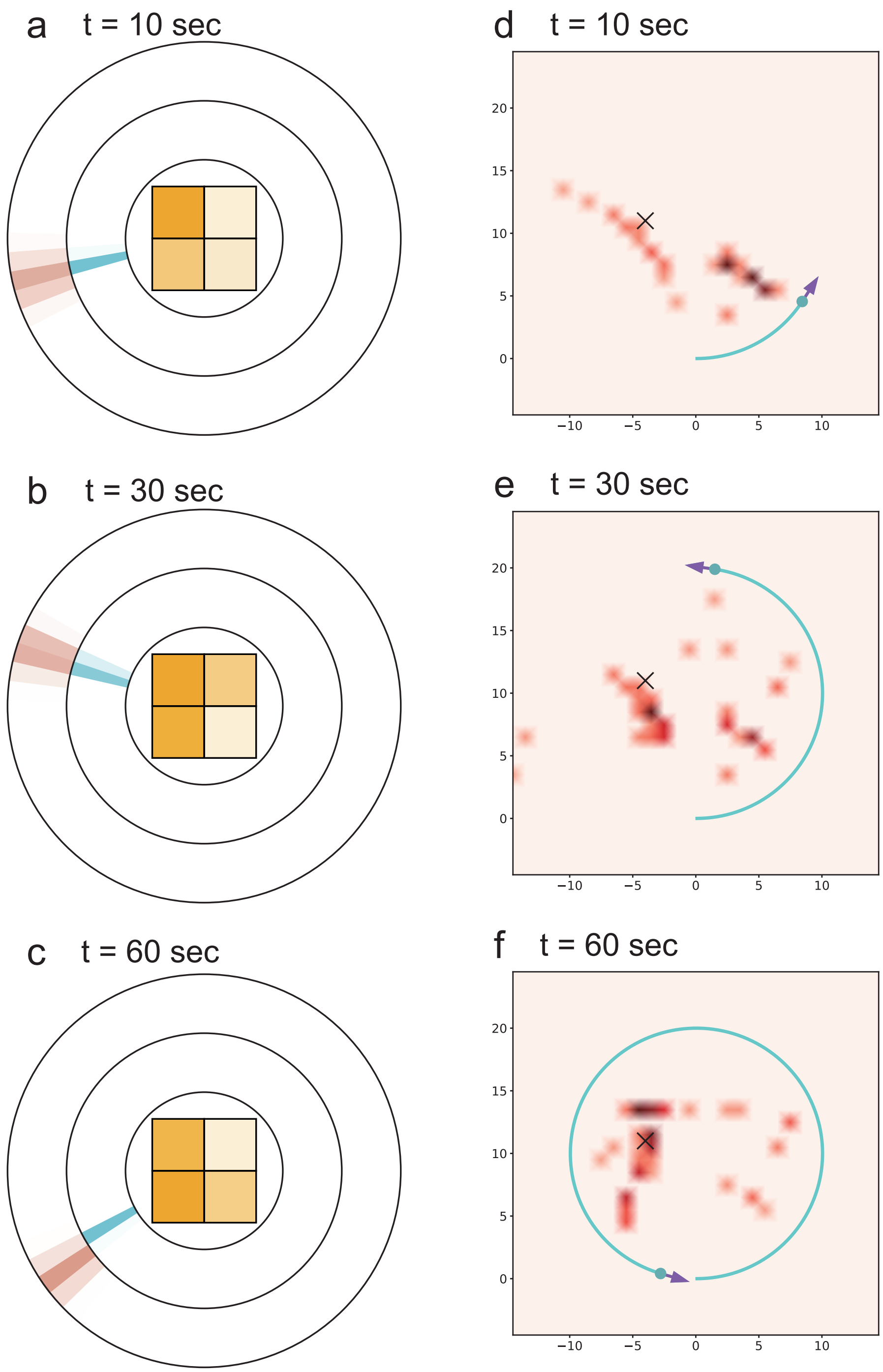

Figure S5. Radiation mapping with a 2×2 square detector.
a-c. The detector's input signals and the predicted direction of the radiation source at t=10, 30, 60 sec. The panel with intense colors represent larger value on the detector's signal. On the pie charts the blue and brown sectors represent the ground-truth and predicted direction of radiation source. The top side of the detector in **a-c.** represents the front side of the moving detector. **d-f.** The process to map the radiation source at t=10, 30, 60 sec. The "×" symbol on the maps show the correct position of the radiation source. The purple arrows indicate the front side of the moving detector. The area with intense red color indicates the sites with high probability to possess radiation source. The unit of length is the meter. Check the radiation mapping process in Supplementary Movie 2.

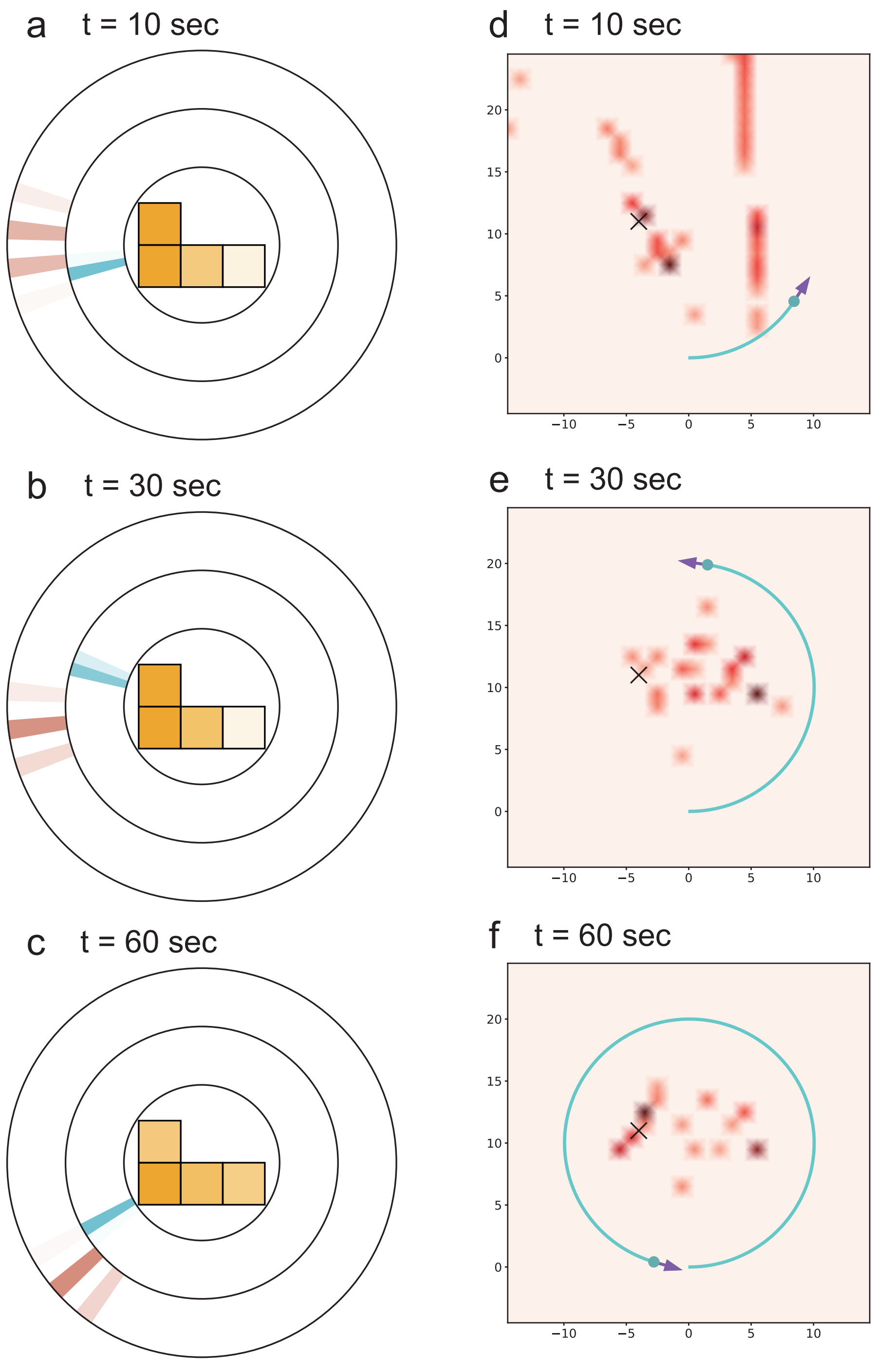

Figure S6. Radiation mapping with a J-shape Tetris-inspired detector.
a-c. The detector's input signals and the predicted direction of the radiation source at t=10, 30, 60 sec. The panel with intense colors represent larger value on the detector's signal. On the pie charts the blue and brown sectors represent the ground-truth and predicted direction of radiation source. The top side of the detector in **a-c.** represents the front side of the moving detector. **d-f.** The process to map the radiation source at t=10, 30, 60 sec. The "×" symbol on the maps show the correct position of the radiation source. The purple arrows indicate the front side of the moving detector. The area with intense red color indicates the sites with high probability to possess radiation source. The unit of length is the meter. Check the radiation mapping process in Supplementary Movie 3.

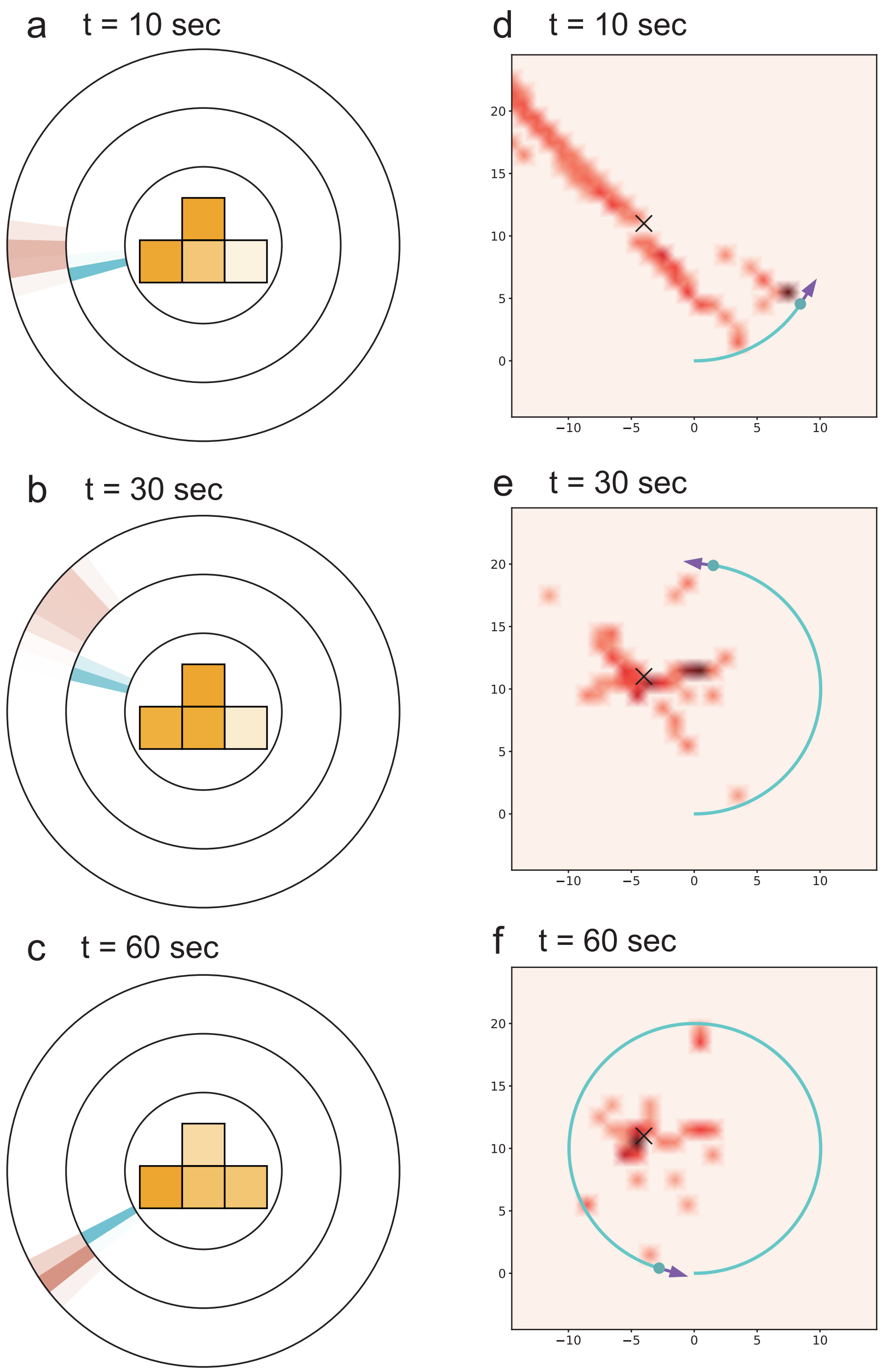

Figure S7. Radiation mapping with a T-shape Tetris-inspired detector.
a-c. The detector's input signals and the predicted direction of the radiation source at t=10, 30, 60 sec. The panel with intense colors represent larger value on the detector's signal. On the pie charts the blue and brown sectors represent the ground-truth and predicted direction of radiation source. The top side of the detector in **a-c.** represents the front side of the moving detector. **d-f.** The process to map the radiation source at t=10, 30, 60 sec. The "×" symbol on the maps show the correct position of the radiation source. The purple arrows indicate the front side of the moving detector. The area with intense red color indicates the sites with high probability to possess radiation source. The unit of length is the meter. Check the radiation mapping process in Supplementary Movie 4.

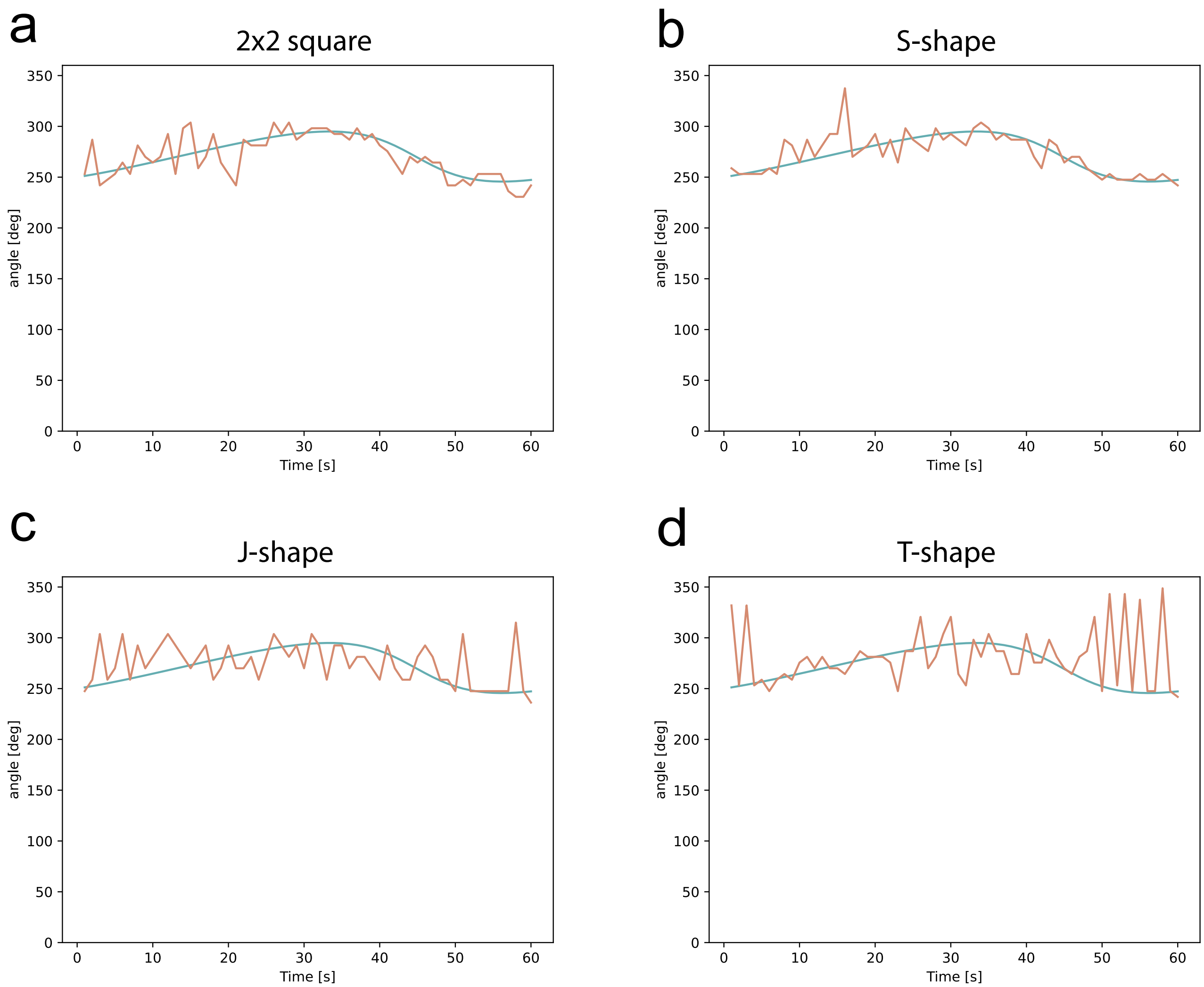

Figure S8. The predicted and actual directions of the radiation source position.
The blue and brown lines track the changes of the actual directions and the predicted directions with detectors of **a.** 2×2 square shape **b.** S-shape **c.** J-shape **d.** T-shape during the radiation mapping process of Figure 3, S5-S7. Here the direction is defined as the clockwise angle from the front side of the detector.

Mapping two radiations sources

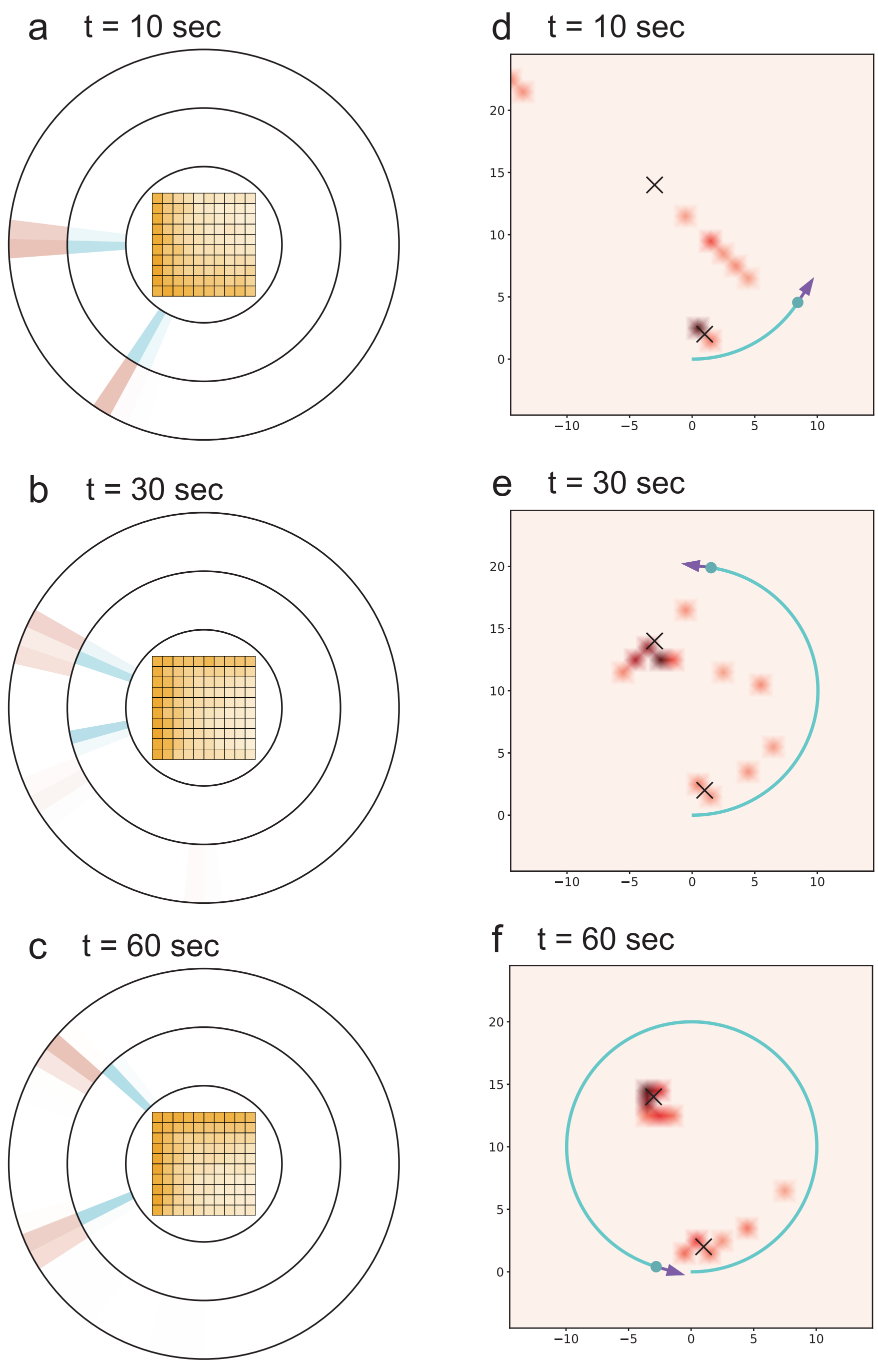

Figure S9. **Mapping 2 radiation sources with a 10×10-size detector.**
a-c. The detector's input signals and the predicted direction of the radiation source at t=10, 30, 60 sec. The panel with intense colors represent larger value on the detector's signal. On the pie charts the blue and brown sectors represent the ground-truth and predicted direction of radiation source. The top side of the detector in **a-c.** represents the front side of the moving detector. **d-f.** The process to map the radiation source at t=10, 30, 60 sec. The "×" symbol on the maps show the correct position of the radiation source. The purple arrows indicate the front side of the moving detector. The area with intense red color indicates the sites with high probability to possess radiation source. The unit of length is the meter. Check the radiation mapping process in Supplementary Movie 5.

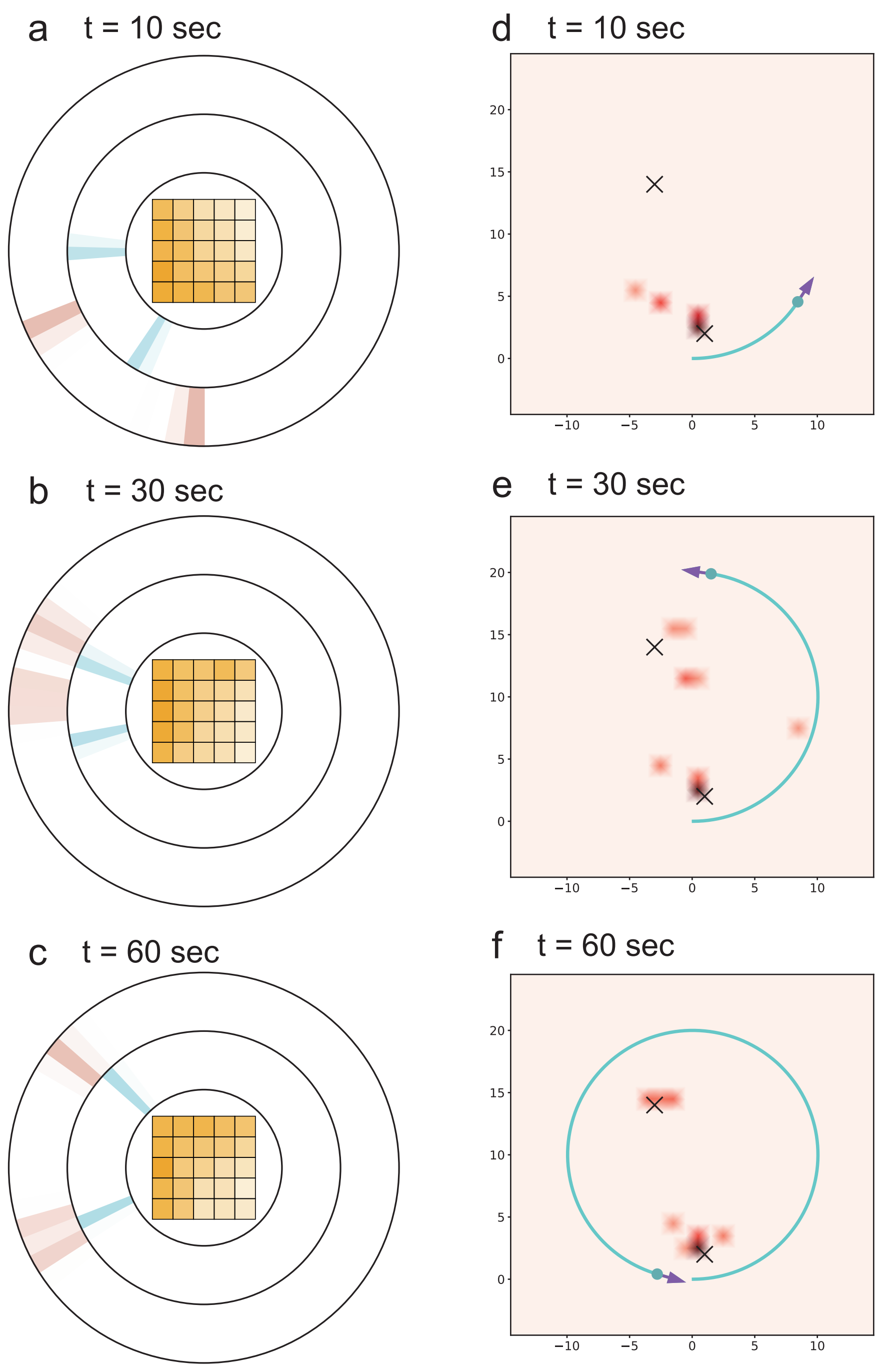

Figure S10. Mapping 2 radiation sources with a 5×5-size detector.
a-c. The detector's input signals and the predicted direction of the radiation source at t=10, 30, 60 sec. The panel with intense colors represent larger value on the detector's signal. On the pie charts the blue and brown sectors represent the ground-truth and predicted direction of radiation source. The top side of the detector in **a-c.** represents the front side of the moving detector. **d-f.** The process to map the radiation source at t=10, 30, 60 sec. The "×" symbol on the maps show the correct position of the radiation source. The purple arrows indicate the front side of the moving detector. The area with intense red color indicates the sites with high probability to possess radiation source. The unit of length is the meter. Check the radiation mapping process in Supplementary Movie 6.

Radiation mapping with a rotating detector moving along the circular trajectory.

In the previous section we have shown that the detectors which are always facing the traveling direction can map radiation sources. However, it is also worthwhile mentioning that the particular detector face that aligns with the detector moving direction does not matter much. The detector facing any direction is already a valid directional detector that is sensitive to radiations coming from all directions. We demonstrate the cases that the moving S-shape detector does not face the traveling direction but rotates at its sites along the circular trajectory. Figure S11 shows how we set up the simulation. As the detector moves along the circular trajectory by angle θ anticlockwise, we rotate the detector by φ anticlockwise. Figure S12-S15 show the mapping results with $\varphi = \theta, 2\theta, -\theta, -2\theta$. Note that $\varphi = \theta$ means the facing side of the detector looks constant from the static observer. We plot the direct predictions of angles in Fig. S16, as we did in the previous section.

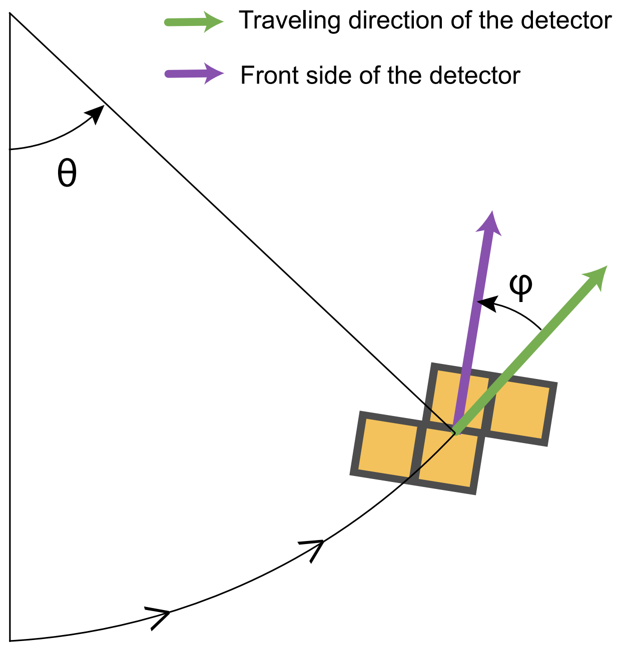

Figure S11. The method to rotate the directional detector when mapping the radiation source distributions.

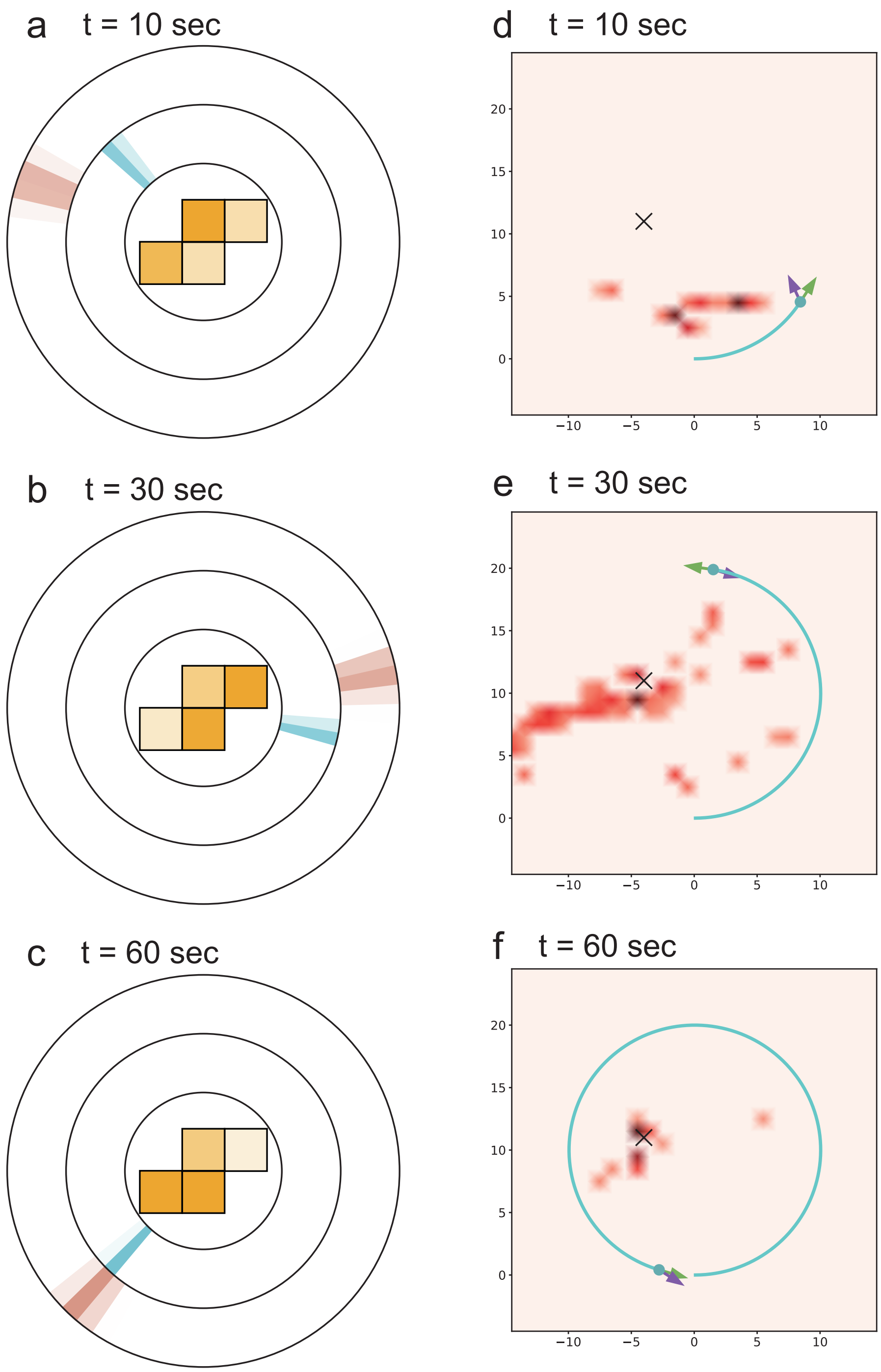

Figure S12. **Radiation mapping with a S-shape Tetris-inspired detector ($\varphi = \theta$).**
a-c. The detector's input signals and the predicted direction of the radiation source at t=10, 30, 60 sec. The panel with intense colors represent larger value on the detector's signal. On the pie charts the blue and brown sectors represent the ground-truth and predicted direction of radiation source. The top side of the detector in **a-c.** represents the front side of the moving detector. **d-f.** The process to map the radiation source at t=10, 30, 60 sec. The "$\times$" symbol on the maps show the correct position of the radiation source. The purple and green arrows indicate the front side of the moving detector and the traveling direction respectively. The area with intense red color indicates the sites with high probability to possess radiation source. The unit of length is the meter. Check the radiation mapping process in Supplementary Movie 7.

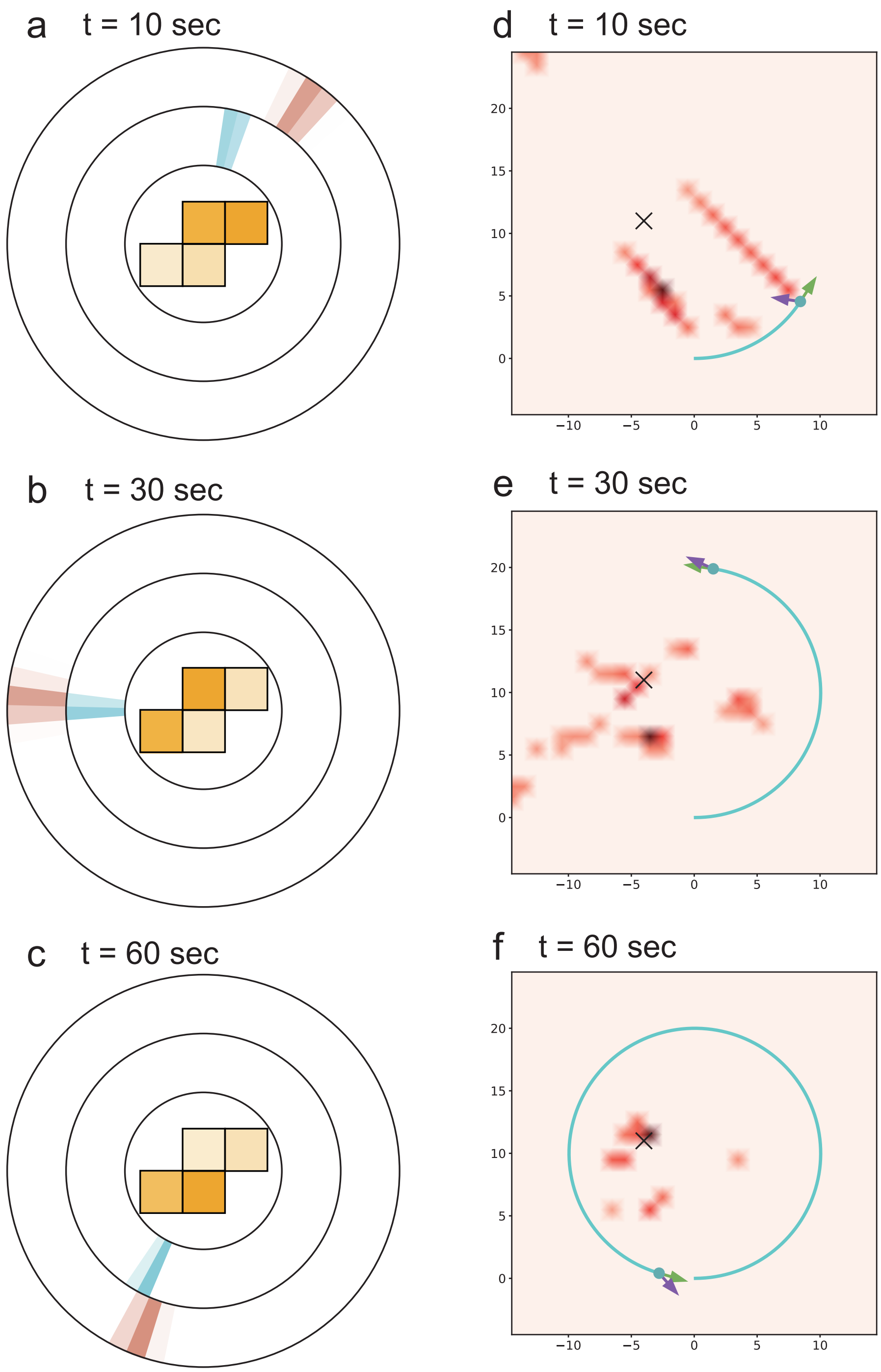

Figure S13. Radiation mapping with a S-shape Tetris-inspired detector ($\varphi = 2\theta$).
a-c. The detector's input signals and the predicted direction of the radiation source at t=10, 30, 60 sec. The panel with intense colors represent larger value on the detector's signal. On the pie charts the blue and brown sectors represent the ground-truth and predicted direction of radiation source. The top side of the detector in **a-c.** represents the front side of the moving detector. **d-f.** The process to map the radiation source at t=10, 30, 60 sec. The "$\times$" symbol on the maps show the correct position of the radiation source. The purple and green arrows indicate the front side of the moving detector and the traveling direction respectively. The area with intense red color indicates the sites with high probability to possess radiation source. The unit of length is the meter. Check the radiation mapping process in Supplementary Movie 8.

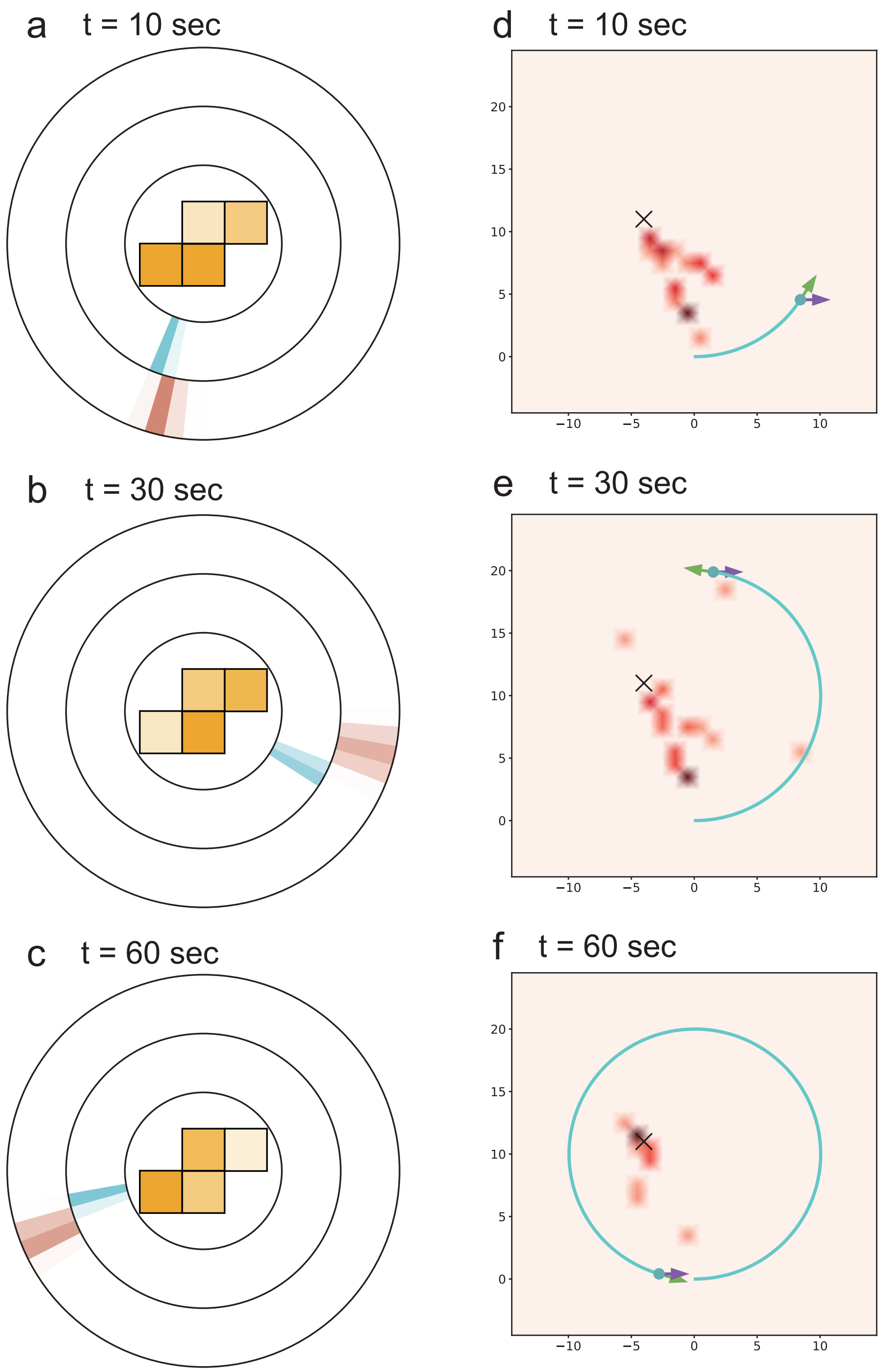

Figure S14. **Radiation mapping with a S-shape Tetris-inspired detector ($\varphi = -\theta$).**
a-c. The detector's input signals and the predicted direction of the radiation source at t=10, 30, 60 sec. The panel with intense colors represent larger value on the detector's signal. On the pie charts the blue and brown sectors represent the ground-truth and predicted direction of radiation source. The top side of the detector in **a-c.** represents the front side of the moving detector. **d-f.** The process to map the radiation source at t=10, 30, 60 sec. The "$\times$" symbol on the maps show the correct position of the radiation source. The purple and green arrows indicate the front side of the moving detector and the traveling direction respectively. The area with intense red color indicates the sites with high probability to possess radiation source. The unit of length is the meter. Check the radiation mapping process in Supplementary Movie 9.

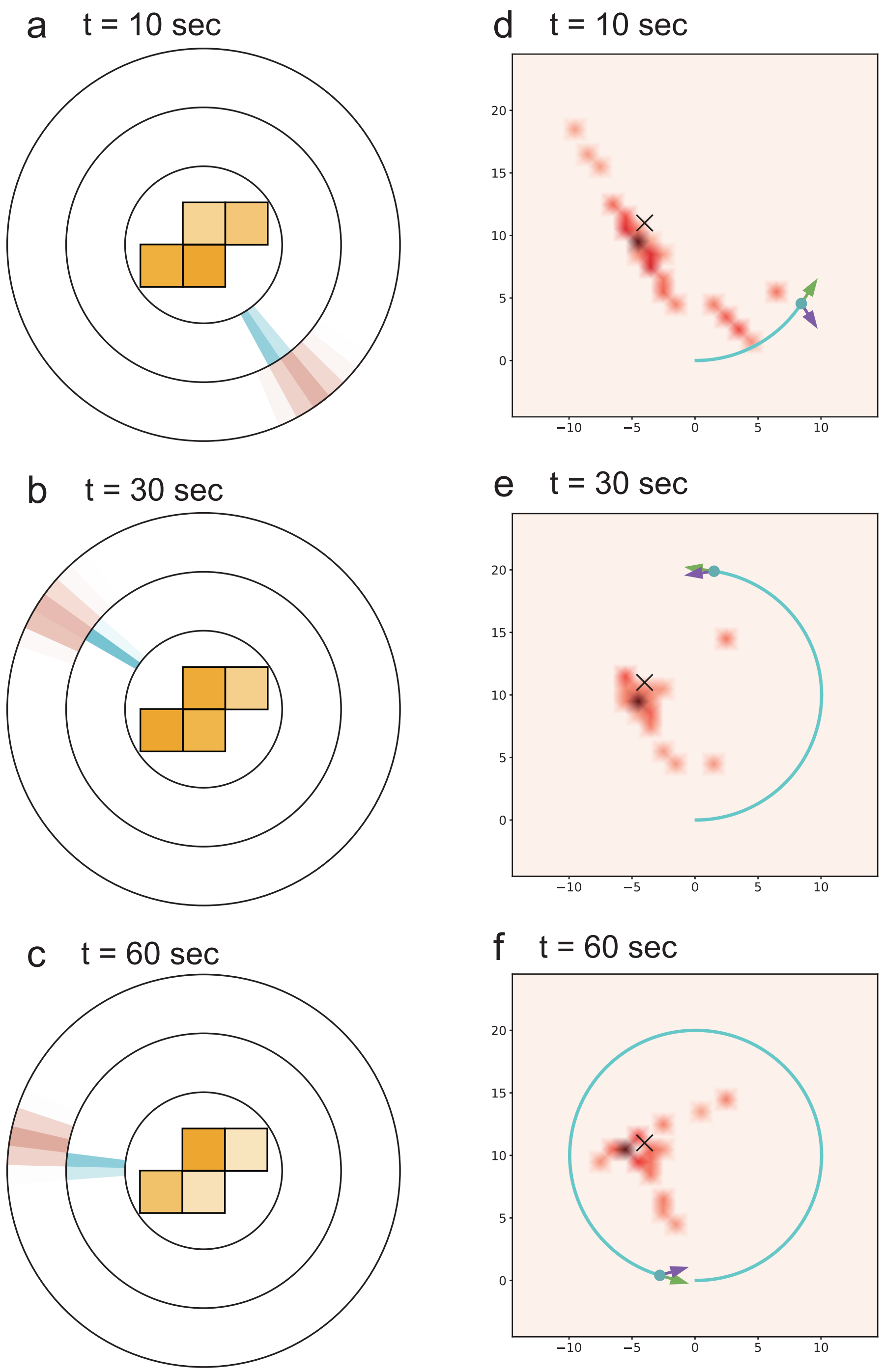

Figure S15. Radiation mapping with a S-shape Tetris-inspired detector ($\varphi = -2\theta$).
a-c. The detector's input signals and the predicted direction of the radiation source at t=10, 30, 60 sec. The panel with intense colors represent larger value on the detector's signal. On the pie charts the blue and brown sectors represent the ground-truth and predicted direction of radiation source. The top side of the detector in **a-c.** represents the front side of the moving detector. **d-f.** The process to map the radiation source at t=10, 30, 60 sec. The "×" symbol on the maps show the correct position of the radiation source. The purple and green arrows indicate the front side of the moving detector and the traveling direction respectively. The area with intense red color indicates the sites with high probability to possess radiation source. The unit of length is the meter. Check the radiation mapping process in Supplementary Movie 10.

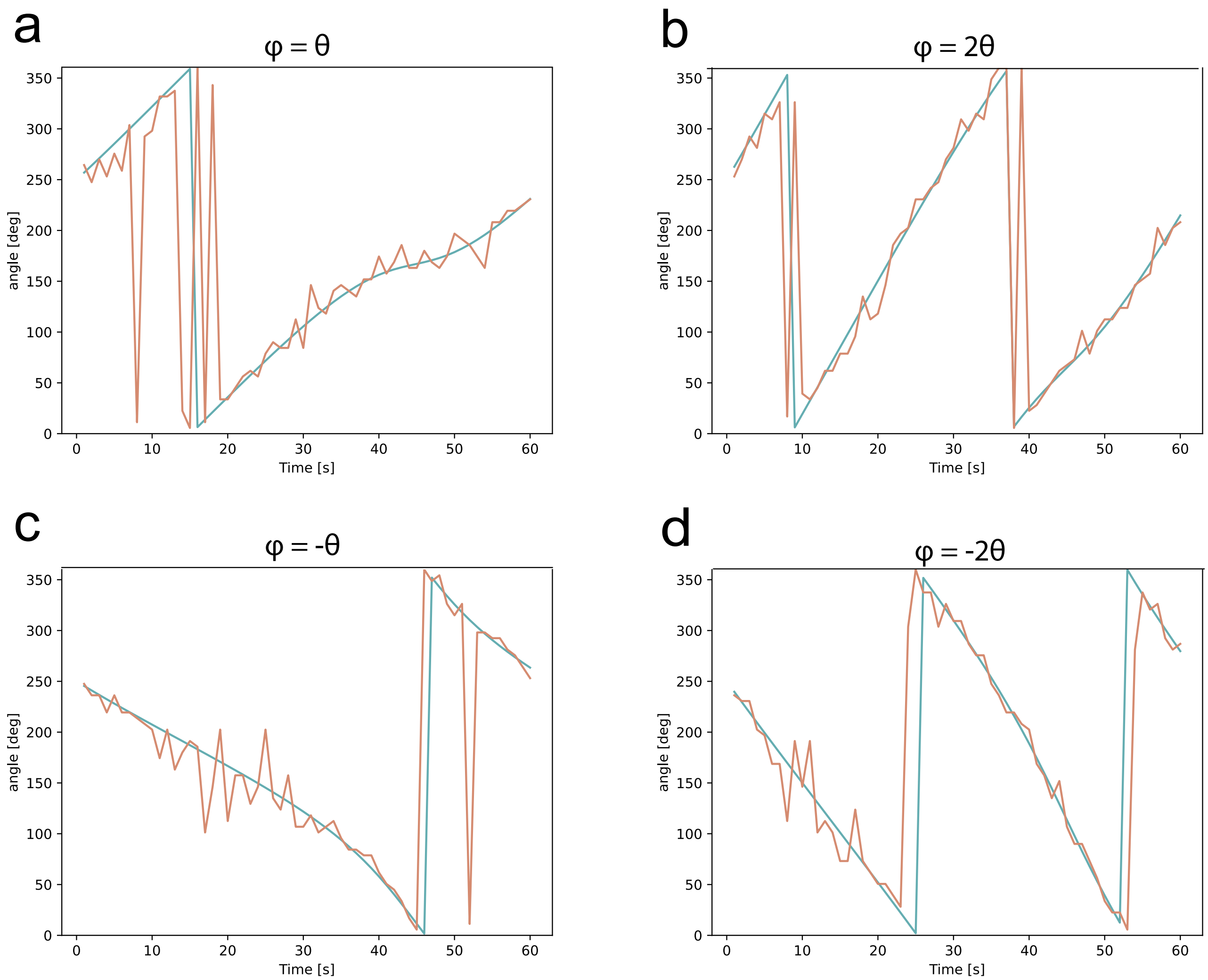

Figure S16. The predicted and actual directions of the radiation source position.
The blue and brown lines track the changes of the actual directions and the predicted directions with detectors of **a.** $\varphi = \theta$, **b.** 2θ, **c.** $-\theta$, **d.** -2θ during the radiation mapping process of Fig. S12-S15. Here the direction is defined as the clockwise angle from the front side of the detector.